ELSEVIER

Journal of Power Sources 111 (2002) 268–282

JOURNAL OF POWER SOURCES

www.elsevier.com/locate/jpowsour

Heat and power management of a direct-methanol-fuel-cell (DMFC) system

H. Dohle*, J. Mergel, D. Stolten

Institut für Werkstoffe und Verfahren der Energietechnik (IWV-3), Forschungszentrum Jülich GmbH, D-52425 Julich, Germany

Received 28 January 2002; received in revised form 9 May 2002; accepted 27 May 2002

Abstract

In this paper, we describe the heat and the power management of a direct methanol fuel cell system. The system consists mainly of a direct methanol fuel cell stack, an anode feed loop with a heat exchanger and on the cathode side, a compressor/expander unit. The model calculations are carried out by analytical solutions for both mass and energy flows. The study is based on measurements on laboratory scale single cells to obtain data concerning mass and voltage efficiencies and temperature dependence of the cell power. In particular, we investigated the influence of water vaporization in the cathode on the heat management of a direct-methanol-fuel-cell (DMFC) system. Input parameters were the stack temperature, the cathode pressure and the air flow rate. It is shown that especially at operating temperatures above 90 °C, the combinations of pressure and air flow rate are limited because of heat losses due to vaporization of water in the cathode.

Keywords: DMFC; Stack; System; Efficiency

1. Introduction

A power system based on a fuel cell is a promising alternative to existing energy conversion techniques [1]. Even at low operating temperatures a better efficiency than, e.g. in conventional power plants or internal combustion engines can be obtained. Because of their low operating temperature the emissions are negligible. Since in a direct-methanol-fuel-cell (DMFC), the methanol is directly fed to the fuel cell, i.e. without an intermediate reformer, DMFC systems have the potential for a particularly simple design and are thus also economically promising. DMFC stacks in the power range of 0.5–1 kW have recently been reported [2,3].

In a direct methanol fuel cell the following catalytically active reactions take place:

$$\text{anode}: \quad CH_3OH + H_2O \Rightarrow CO_2 + 6H^+ + 6e^-$$

$$\text{cathode}: \quad 6H^+ + 6e^- + 1.5O_2 \Rightarrow 3H_2O$$

$$\text{overall reaction}: \quad CH_3OH + 1.5O_2 \Rightarrow CO_2 + 2H_2O$$

The theoretical open circuit voltage (U_0) of a DMFC is calculated from the free Gibbs enthalpy (ΔG) of the overall reaction:

$$\Delta G = \Delta H - T\Delta S \tag{1.1}$$

ΔG is the maximum amount of energy which can be converted into work. It is derived from the heating value (ΔH) of the fuel less the change of entropy (ΔS) multiplied by the temperature (T). ΔG is distributed on the electrons participating the overall reaction by means of a potential difference between the anode and the cathode. The theoretical open circuit voltage (U_0) is at the same time the theoretical maximum possible voltage which is defined by thermodynamic laws. It can be calculated from ΔG divided by the number (n) of the electrons transferred during the reaction and the Faraday constant (F):

$$U_0 = \frac{\Delta G}{nF} \quad \text{with } n = 6 \text{ and } F = 96485\,\text{A s/mol} \tag{1.2}$$

Due to overpotentials at the anode as well as at the cathode the open circuit voltage under real conditions is always lower than the theoretical value depending on the catalysts, the electrolyte and the kind of fuel used.

The thermoneutral voltage (U_{th}) thus follows as:

$$U_{th} = \frac{\Delta H}{6F} \tag{1.3}$$

* Corresponding author.
E-mail address: h.dohle@fz-juelich.de (H. Dohle).

0378-7753/02/$ – see front matter
PII: S0378-7753(02)00339-7

Nomenclature

c_p	heat capacity
F	Faraday constant (96,485 A s/mol)
ΔG	free Gibbs enthalpy
ΔH	heating value
ΔH_V	evaporation enthalpy of water
I_{el}	electric current
I_{perm}	methanol permeation expressed as a parasitic current
n	number of electrons involved in reaction
n_p	polytropic exponent
N_{air}	molar flow of air (mol/s)
N_{CO_2}	molar flow of carbon dioxide (mol/s)
$N_{MeOH,el}$	molar flow of methanol due to electric current (mol/s)
$N_{MeOH,perm}$	molar flow of methanol due to permeation (mol/s)
$N_{MeOH,total}$	total molar flow of methanol (mol/s)
N_{N_2}	molar flow of nitrogen (mol/s)
N_{O_2}	molar flow of oxygen (mol/s)
p	absolute pressure (bar)
p^*	reference pressure (bar)
p_{total}	total pressure (bar)
P_{aux}	power demand of the auxiliary components (W)
P_{cell}	fuel cell power output (W)
P_{compr}	compressor work (W)
P_{exp}	expander work (W)
Q	heat (J)
R	molar gas constant
ΔS	change of entropy
T	temperature
T^*	reference temperature
U_0	reversible cell voltage (V)
U_C	cell voltage (V)
U_{th}	thermoneutral cell voltage (V)
w_{pol}	polytropic work (J/mol)
x	molar fraction
Z	number of compressor stages

Greek symbols

η_{aux}	efficiency of the auxiliary components
$\eta_{c,e}$	efficiency of the compressor and the expander
η_{fc}	fuel cell efficiency
η_L	load efficiency
η_q	thermal efficiency
η_{system}	system efficiency
η_{th}	thermodynamic efficiency
η_U	voltage efficiency
λ	stoichiometric factor
ν	stoichiometric factor related to current generation
χ	parameter of the equation of Clausius–Clapeyron

Superscripts and subscripts

in	incoming
out	outgoing
liq.	liquid phase
gas	gas phase

U_{th} defines a fictitious cell voltage with no heat transfer from or into the fuel cell. Bringing U_0 and U_{th} into correlation, the thermodynamic efficiency of a fuel cell is obtained as:

$$\eta_{th} = \frac{U_0}{U_{th}} = \frac{\Delta G}{\Delta H} = 1 - \frac{T\Delta S}{\Delta H} \tag{1.4}$$

In the case of the DMFC the theoretical efficiency for standard conditions ($T = 25\ ^\circ C$, $p = 1.013$ bar) is almost 100% (Table 1).

The cell potential during operation is affected by Ohmic losses, overvoltages at the electrodes and by the formation of a mixed potential at the cathode. Especially the low kinetics of the DMFC anode is responsible for substantially higher overvoltages (approximately 200–300 mV) in comparison to the hydrogen anodes of PEM fuel cells. The mixed potential at the cathode lowers the cell voltage in the range of 50–200 mV depending on the operating conditions as temperature and methanol concentration [4]. The voltage efficiency (η_U) is the ratio of the cell voltage (U_C) during operation to the theoretical open circuit potential:

$$\eta_U = \frac{U_C}{U_0} \tag{1.5}$$

Finally, a load efficiency (η_L) can be defined from the ratio of the cell voltage (U_C) and the thermoneutral voltage (U_{th}):

$$\eta_L = \frac{U_C}{U_{th}} \tag{1.6}$$

Fig. 1 shows the basic processes in a DMFC. Methanol is consumed due to two processes. The first one is of course the electrochemical conversion of methanol into electric current whereas the second process is the methanol permeation from the anode to the cathode. Methanol permeation causes losses due to additional methanol consumption and due to the formation of a mixed potential at the cathode decreasing the cell power [5].

The overall methanol consumption is:

$$N_{MeOH,total} = N_{MeOH,el} + N_{MeOH,perm} \tag{1.7}$$

According to Faraday's law, $N_{MeOH,el}$ can be expressed as:

$$N_{MeOH,el} = \frac{I_{el}}{6F} \tag{1.8}$$

The methanol permeation ($N_{MeOH,perm}$) can be expressed as a corresponding parasitic current (I_{perm}) using Faraday's law:

$$N_{MeOH,perm} = \frac{I_{perm}}{6F} \tag{1.9}$$

Table 1
Comparison of the thermodynamic data of H_2 PEM and DMFC

Reaction	Temperature (°C)	ΔH (kJ/mol)	ΔS (J/mol K)	ΔG (kJ/mol)	U_0 (V)	η_{th}
$H_2 + \frac{1}{2}O_2 \rightarrow H_2O_{(liq.)}$	25	−285.8	−162.4	−237.4	1.23	0.83
$CH_3OH_{(liq.)} + \frac{3}{2}O_2 \rightarrow CO_2 + 2H_2O_{(liq.)}$	25	−726.3	−80.2	−702.4	1.21	0.97

The mass efficiency (η_M) defines the ratio of the methanol flow ($N_{MeOH,el}$) which is used to generate the electric current (I_{el}) to the overall flow of methanol ($N_{MeOH,total}$) with:

$$\eta_M = \frac{N_{MeOH,el}}{N_{MeOH,total}} = \frac{N_{MeOH,el}}{N_{MeOH,el} + N_{MeOH,perm}} \quad (1.10)$$

or using Eqs. (1.8) and (1.9):

$$\eta_M = \frac{I_{el}}{I_{el} + I_{perm}} \quad (1.11)$$

There are two causes of methanol permeation from the anode to the cathode: the first one is the diffusion of methanol from the anode to the cathode and second, the methanol transport by electro-osmosis. The cause of the methanol diffusion is the concentration gradient through the membrane which is maintained by the oxidation of methanol reaching the cathode. The amount of solvated methanol molecules transported by electro-osmosis is mainly a function of the current density, the methanol concentration at the interface between the anode electrode and the membrane as well as the membrane properties [6].

The product of the mass efficiency and the load efficiency:

$$\eta_{fc} = \eta_M \eta_L \quad (1.12)$$

is defined as the overall efficiency of the fuel cell.

2. Evaluation of a DMFC system

In addition to determining the electric power it is necessary to balance the heat fluxes in order to obtain the quantity and temperature level of the recoverable heat. This heat can be taken easily from the anode loop. The heat generation not only influences the temperature gradient and power gradient in the stack [7,8] but also the design of the auxiliary components as described below.

Fig. 2 shows a DMFC system scheme. The air reaches the cathode compartment via a compressor/expander unit. The exhaust gases from both the anode and cathode side are additionally passed through a catalytic burner to remove organic components.

In the system depicted, cooling is effected via a heat exchanger in the anode loop. On the cathode side a separator serves both to recycle the water which has reached the

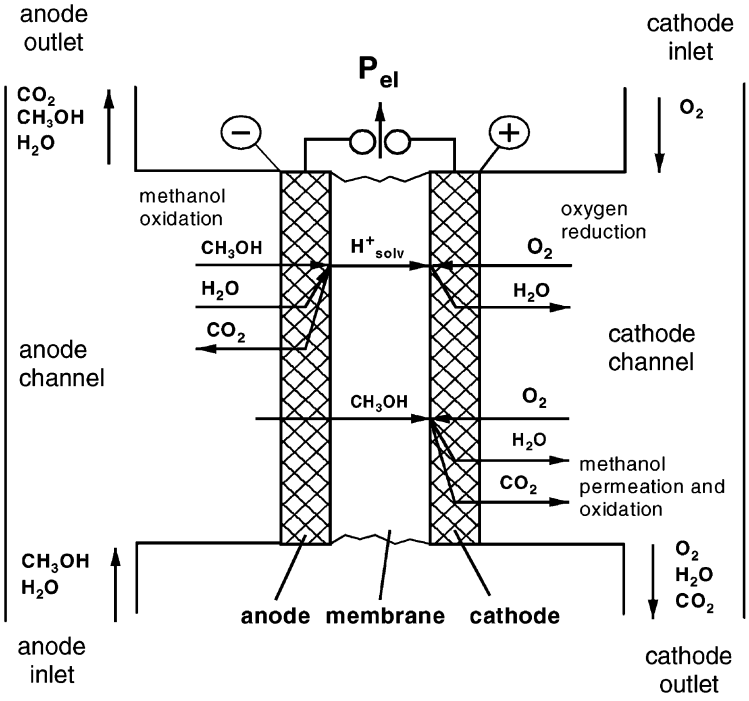

Fig. 1. Basic scheme of the DMFC.

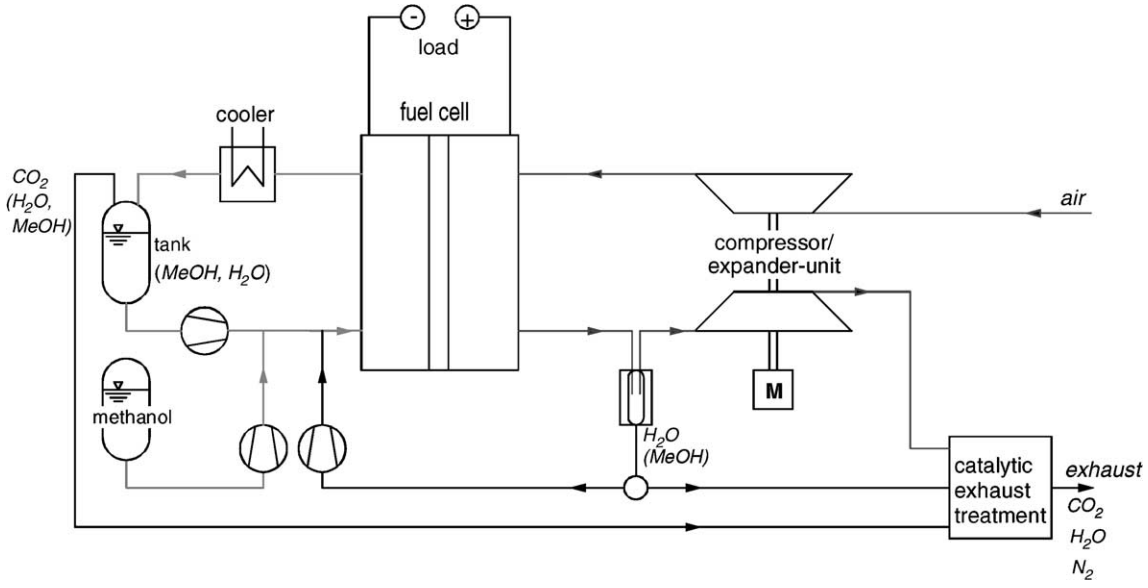

Fig. 2. DMFC system with air.

cathode by electro-osmosis as well as to separate the product water from the exhaust gas stream.

The fuel cell system consists of additional auxiliary components such as pumps or compressors which are driven by the fuel cell. The fuel cell itself generates the power (P_{cell}), whereas the auxiliary components consume the additional power ($\sum P_{\text{aux}}$).

The expression:

$$\eta_{\text{aux}} = \frac{P_{\text{cell}} - \sum P_{\text{aux}}}{P_{\text{cell}}} \tag{2.1}$$

as an efficiency of the auxiliary system components compared to the fuel cell power output (P_{cell}) and in addition defining:

$$\eta_{\text{system}} = \left(\frac{P_{\text{cell}} - \sum P_{\text{aux}}}{P_{\text{cell}}}\right)\eta_{\text{fc}} \tag{2.2}$$

leads to an expression for the overall system efficiency, including the fuel cell and the auxiliary components. The fuel cell efficiency (η_{fc}) depends on the cell voltage and the fuel utilization as summarized in Eq. (1.12).

2.1. Volume flows

In a liquid-operated DMFC the membrane is always almost saturated so that water can easily vaporize into the cathode compartment.

2.1.1. Cathode

In order to determine the necessary power demand of the compressor/expander unit it is necessary to determine the volume flows:

2.1.1.1. Incoming volume flows. The stoichiometric air flow rate (λ) defines the inlet air flow:

$$N_{\text{air,in}} = \lambda \frac{1}{x_{O_2}} \frac{I_{\text{el}}}{4F} \tag{2.3}$$

The molar flow of air entering the cathode ($N_{\text{air,in}}$) with the oxygen molar fraction (x_{O_2}) is consumed by current generation and methanol permeation. The introduction of a stoichiometric factor (v), related to the current generation, yields:

$$N_{\text{air,in}} = \frac{1}{x_{O_2}} \left(v\left(\frac{I_{\text{el}}}{4F}\right) + \frac{I_{\text{perm}}}{4F} \right) \tag{2.4}$$

The factor v consequently specifies how many times the volume of oxygen is available for actual current generation in addition to that consumed by methanol permeation.

Substituting the relation (1.11) for the mass efficiency (η_{M}) yields the air ratio (λ):

$$\lambda = \frac{1}{\eta_{\text{M}}} + (v - 1) \tag{2.5}$$

Electricity can only be produced if:

$$v \geq 1 \tag{2.6}$$

The minimum air ratio necessary (λ_{min}), therefore, only depends on the mass efficiency:

$$\lambda_{\text{min}} \geq \frac{1}{\eta_{\text{M}}} \tag{2.7}$$

2.1.1.2. Outgoing volume flows. Balancing of the gas molar flows leaving the cathode compartment yields:

$$N_{O_2,\text{out}} = \frac{I_{\text{el}}}{4F}(v - 1) \tag{2.8}$$

The outgoing nitrogen flow corresponds to the nitrogen molar flow entering the channel:

$$N_{N_2,\text{out}} = \frac{x_{N_2,\text{in}}}{x_{O_2,\text{in}}} \frac{I_{\text{el}}}{4F} \left[\frac{1}{\eta_{\text{M}}} + (v - 1) \right] \tag{2.9}$$

$$N_{CO_2,out} = \frac{I_{el}}{6F}\left[\frac{1}{\eta_M} - 1\right] \tag{2.10}$$

The outgoing volume flow is assumed to be saturated with water vapor. The fraction x_{H_2O} corresponds to:

$$x_{H_2O} = \frac{p_{H_2O}}{p_{total}} \tag{2.11}$$

The partial pressure of the saturated water vapor (p_{H_2O}) as a function of the temperature (T) follows in good approximation the equation of Clausius–Clapeyron [9]:

$$p_{H_2O} = p^* \, e^{-\chi} \quad \text{with } \chi = \frac{\Delta H_V}{R}\left(\frac{1}{T} - \frac{1}{T^*}\right),$$
$$\text{where } p^* = 1 \text{ bar}; \; T^* = 373.15 \text{ K} \tag{2.12}$$

In Eq. (2.12), the boiling point of water at atmospheric pressure (p^*) and temperature (T^*) is used as a reference. In general, the equation of Clausius–Clapeyron is applicable for calculating the saturated vapor pressure of liquids in a specific temperature range if:

- the evaporation enthalpy ΔH_V is nearly constant in the relevant temperature range, i.e. $\Delta H_V(T) = \Delta H_V =$ constant;
- the specific volume of the liquid phase is negligible compared to that of the gas phase;
- the saturated vapor phase can be treated as an ideal gas.

All conditions are fulfilled for water in the temperature range from 60 to 130 °C with an evaporation enthalpy (ΔH_V) of approximately 40 kJ/(mol K) and the specific volume of the gas phase being three orders of magnitude higher than that of the liquid phase [9].

Hence, follows the gaseous water molar flow leaving the cathode compartment:

$$N_{H_2O,out} = \frac{x_{H_2O}}{1 - x_{H_2O}}\left(N_{CO_2,out} + N_{N_2,out} + N_{O_2,out}\right) \tag{2.13}$$

or with Eqs. (2.8)–(2.10):

$$N_{H_2O,out} = \frac{x_{H_2O}}{1 - x_{H_2O}}\frac{I_{el}}{4F}\left[v\left(1 + \frac{1 - x_{O_2,in}}{x_{O_2,in}}\right) + \frac{1}{\eta_M}\left(\frac{1 - x_{O_2,in}}{x_{O_2,in}} + \frac{2}{3}\right) - \left(\frac{5}{3} + \frac{1 - x_{O_2,in}}{x_{O_2,in}}\right)\right] \tag{2.14}$$

The pressure changes from p_1 to p_2 in the compressor as well as in the expander are assumed to be polytropic. The specific compression or expansion work (w_{pol}) for polytropic changes of state is [9]:

$$w_{pol} = Z c_p T_{in}\left[\left(\frac{p_2}{p_1}\right)^{(1/Z)((n_p-1)/n_p)} - 1\right] \tag{2.15}$$

where Z is the number of compressor stages ($Z = 1$), c_p the specific heat capacity, T_{in} the inlet temperature ($T_{in} = 298$ K), n_p the polytropic exponent ($n_p = 1.5$), p_1 the compressor/expander inlet pressure (1 bar) and p_2 the compressor/expander outlet pressure, and multiplied by the corresponding gas molar flows at the cathode inlet and outlet.

An efficiency ($\eta_{c,e}$) of 80% is assumed for both the compressor and the expander. Phase changes in the expander are not taken into consideration.

2.1.2. Anode

The volume flow on the anode side influences the formation of a concentration gradient between the anode inlet and the cathode outlet. Low volume flows lead generally to high concentration gradients. To ensure a rather homogeneous operation on the whole area a high volume flow is required.

2.2. Heat balance

The heat balance is based on the following assumptions.

- Complete saturation of the gas mixture with water vapor takes place on the cathode side.
- Temperature gradients inside the cell, especially between the anode and cathode, are negligible.
- Methanol reaching the cathode is completely oxidized. This assumption is of importance as it implies that the permeated methanol is not recoverable and fully converted into heat. This point has been investigated carefully in Section 3.
- The vaporization enthalpy (ΔH_V) of water for the temperature range of 60–130 °C is assumed to be constant at 40 kJ/mol.

For completeness it is assumed that the anode pressure is the same as at the cathode. The pressure can easily created by the carbon dioxide generation at the anode and adjusted by means of a pressure controller without any additional energy demand. Furthermore, the operation without a pressure gradient across the membrane avoids additional mechanical stress.

Balancing the cell power, the consumed power of the compressor/expander unit, and the incoming and outgoing enthalpy flows leads to:

$$\underbrace{P_{cell} + P_{compr} + P_{exp}}_{\text{system}} + \dot{Q} = \sum \dot{H}_{out} - \sum \dot{H}_{in} \tag{2.16}$$

The electric power of the cell is:

$$P_{cell} = U_C I_{el} = \eta_L U_{th} I_{el} \tag{2.17}$$

The difference of the incoming and outgoing enthalpy flow ($\sum \dot{H}_{out} - \sum \dot{H}_{in}$) is mainly caused by the consumption of methanol and by the vaporization of water at the cathode:

$$\sum \dot{H}_{out} - \sum \dot{H}_{in} = U_{th}(I_{perm} + I_{el}) + N^{gas}_{H_2O,out}\,\Delta H_V \tag{2.18}$$

with ΔH_V expressing the vaporization enthalpy of water. The enthalpy difference between the incoming and outgoing

molar flows is, therefore:

$$\sum \dot{H}_{\text{out}} - \sum \dot{H}_{\text{in}} = U_{\text{th}} \frac{1}{\eta_{\text{M}}} I_{\text{el}} + N^{\text{gas}}_{\text{H}_2\text{O,out}} \Delta H_{\text{V}} \tag{2.19}$$

The heat flow ($\dot{Q}$) transferred across the system boundary is, therefore, composed of the internal power dissipation:

$$\dot{Q} = \left(\frac{1}{\eta_{\text{M}}} - \eta_{\text{L}} \right) U_{\text{th}} I_{\text{el}} - N^{\text{gas}}_{\text{H}_2\text{O,out}} \Delta H_{\text{V}} \tag{2.20}$$

Eq. (2.20) contains the borderline case of a disappearing heat flux at $\eta_{\text{M}} = 1$, $\eta_{\text{L}} = 1$ and $N^{\text{gas}}_{\text{H}_2\text{O}} = 0$. This corresponds to a fictitious operation of the cell without methanol permeation at the thermoneutral voltage without water vaporization.

The efficiency (η_q):

$$\eta_q = \frac{Q}{\Delta H} \tag{2.21}$$

evaluates the thermally useful energy (Q) relative to the heating value of methanol.

3. Experimental

Current/voltage measurements at the membrane electrode assemblies (MEAs) on a laboratory scale serve to determine the efficiencies and performances defined above. The active surfaces of the MEAs studied are in each case 20 cm^2. The mass efficiency as a function of operating conditions is determined by measuring the methanol permeation, along with an analysis of the carbon dioxide content in the cathode exhaust air.

3.1. Manufacturing of membrane electrode assemblies

The MEA consists of a polymer membrane, anode and cathode catalyst layers and gas diffusion layers. In the following, we briefly describe the manufacturing of the MEAs.

The MEAs used for the experiments were fabricated in-house. We used Nafion 117 as membrane material. Both the anode and cathode gas diffusion layers were prepared by mixing carbon powder with finely-dispersed PTFE. With regard to the different mass transport properties of the electrodes the PTFE content is 10% in the anode to ensure a sufficient transport of liquid methanol and water to the catalyst layer and 40% in the cathode for an improved hydrophobicity for product water removal [10]. The mixture was then applied to a carbon cloth with a loading of approximately 5 mg/cm^2 with a subsequent sintering process at 350 °C.

The anodic catalyst loading is 4 mg/cm^2 carbon-supported Pt/Ru with an atomic ratio of 1:1; cathodic loading is 4 mg/cm^2 Pt-black. The anode catalyst layer was prepared by a spraying method whereas the cathode was prepared by a decal method. The decal methanol is based on three steps:

1. mixing the catalyst with a Nafion solution and applying it to a PTFE foil;
2. drying at 80 °C;
3. hot-pressing of the catalyst layer onto the membrane at 130 °C, 0.5 kN/cm^2, 5 min;
4. removal of the PTFE foil.

In contrast to the cathode catalyst layer, the anode was prepared by the application of the catalyst on the diffusion layer with subsequent hot-pressing onto the membrane. Additional information about preparation and optimization of MEAs is given in [11].

3.2. Test rig

The configuration of the laboratory cell, the test rig shown in Fig. 3 and the exhaust air analysis are described in detail in [12]. The main components of the anode side are the circulation tank, the circulation pump and a CO_2 separator. A defined anode pressure can be adjusted by pressurized nitrogen.

On the cathode side, the test rig mainly consists of the gas supply and the devices for the methanol permeation measurement. The methanol permeation measurement is based on the analysis of the CO_2 content of the cathode exhaust gas stream. A CO_2 sensor (Vaisala GMN 12A) serves for measuring the CO_2 concentration of the cathode exhaust gas. A heated catalytic afterburner can be switched between cell and condenser to oxidize any methanol leaving the cathode compartment unoxidized.

The afterburner consists of a heated tube, which is filled with catalyst material and exhibits a temperature of 230 °C during operation. Pellets of 0.5% Pd on Al_2O_3 are used as the catalyst. In recent experiments, we found that depending on the operating conditions 80–100% of the methanol reaching the cathode is oxidized by the Pt catalyst in the cathode layer. With the experimental setup described above, this amount could easily be measured by comparing the CO_2 signal of the sensor in operation with and without catalytic burner [13]. The development of methanol tolerant cathode materials is, therefore, an important task to circumvent the mixed potential and the methanol losses at the cathode [14].

3.3. Influence of methanol concentration

The methanol concentration on the anode side has a decisive influence on the current/voltage characteristic of a DMFC. Too high a methanol concentration leads to high methanol permeation so that methanol is oxidized at the cathode. The methanol permeation does not only reduce the mass efficiency but is furthermore also responsible for the formation of a mixed potential at the cathode, which reduces the cell voltage and thus decreases the voltage efficiency [15,16].

On one hand, too low a methanol concentration prevents methanol losses and the formation of a mixed potential, but,

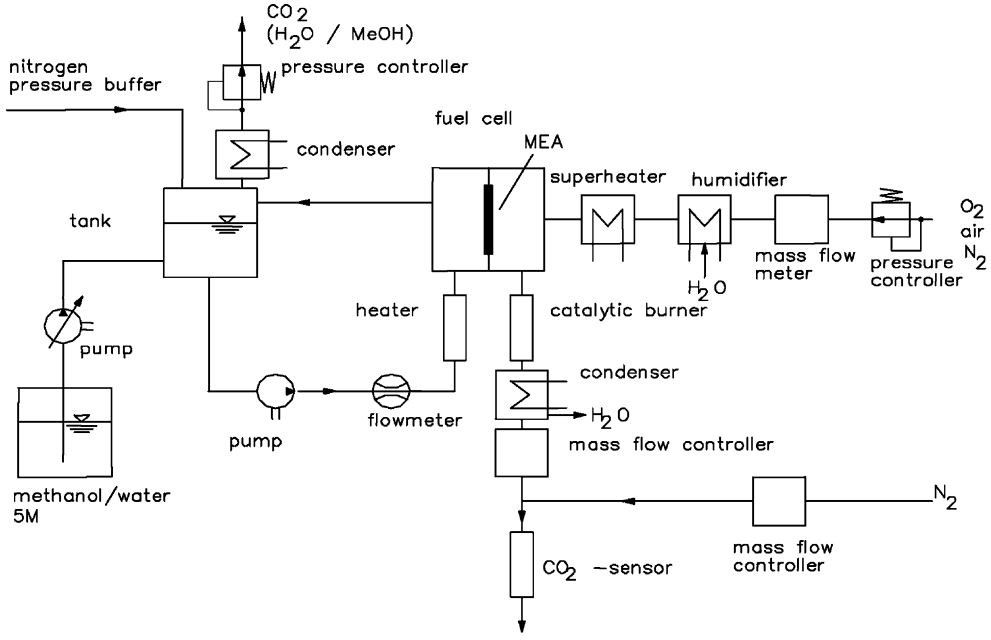

Fig. 3. DMFC test rig.

on the other hand, it is associated with a rise in anodic diffusion overvoltages [17]. Fig. 4 shows the current/voltage characteristics of a DMFC where the methanol concentration is varied. The lowest methanol concentration of 0.5 M shown leads to overvoltages in the high current density range (>300 mA/cm^2) which reduce the cell voltage. At the same time, due to reduced mixed potential formation, the cell voltage is greatest in the low current density range (<200 mA/cm$^{2)}$. The concentration must, therefore, be adjusted to an optimum value representing the best possible compromise with respect to the anodic and cathodic overvoltages.

Measurements of the methanol permeation rate are given in Fig. 5. According to Faraday's law, the permeation rate is expressed as an equivalent current density. Basically, the methanol permeation is caused by diffusion through the membrane and by an additional electro-osmotic drag due to the proton transport through the membrane [6,15]. On one hand, the diffusive fraction of the methanol permeation is caused by a concentration difference between the anode and the cathode. The concentration gradient is maintained by the oxidation of methanol at the cathode. On the other hand, the electro-osmotic fraction is mainly influenced by the current density and the methanol concentration in the interface between anode catalyst layer and membrane [13]. As expected, the methanol permeation increases with increasing methanol concentration. Increasing the current density leads to an elevated fuel consumption in the anodic catalyst layer, i.e. the methanol concentration in the catalyst layer decreases. In the concentration range of 0.5–2 M the

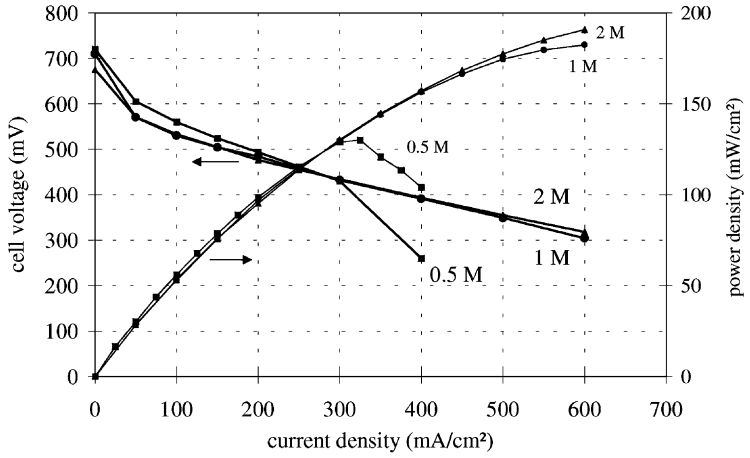

Fig. 4. Current/voltage characteristics for different methanol concentrations. Catalyst loading: anode side, 4 mg/cm^2 Pt/Ru on XC72; cathode side, 4 mg/cm^2 Pt-black. Operating conditions: 110 °C; pressure, 3 bar absolute; oxygen as the oxidant; measuring time per point, 15–30 min.

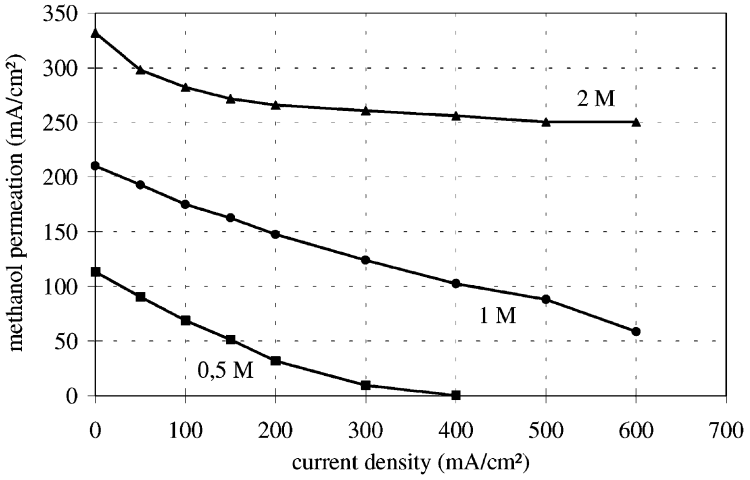

Fig. 5. Methanol permeation for different methanol concentrations. The methanol permeation is expressed as the parasitic current density. Operating conditions: 110 °C; pressure, 3 bar absolute; oxygen as the oxidant; measuring time per point, 15–30 min.

permeation rate decreases with increasing current density. This effect is explained by the elevated fuel consumption in the anodic catalyst layer, so that less methanol is transmitted to the cathode. Fig. 6 shows the relation between the power density and the mass efficiency (η_M). Two kinds of limitations are demonstrated.

1. *Power limitation at low methanol concentration*: Low methanol concentrations (e.g. 0.5 M) lead to a lack of methanol in the anode catalyst layer beginning at relatively low current densities in the range of 350–400 mA/cm^2. The rapid decrease of the cell voltage is caused by the formation of diffusion overvoltages. On the other hand, the lack of methanol in the catalyst layer is advantageously accompanied by very low methanol permeation rates. These correspond directly to high mass efficiencies in the range above 90%.
2. *Mass efficiency limitation at high power densities*: The maximum power density is obtained with a 2 M methanol solution. The relatively high amount of methanol to avoid diffusion overvoltages in the anode is the reason for the lower mass efficiency in the range of 70% at maximum cell power.

For further system studies, two design points are defined in the following.

- *Full power range*: This is the range in which the fuel cell supplies its greatest power. The cell voltage of a single cell is about 300 mV.
- *Partial power range*: This corresponds to a single cell voltage of 500 mV. The partial power is about 50% of the full power.

An important issue for evaluating the system characteristics is the air demand. The maximum air demand defines

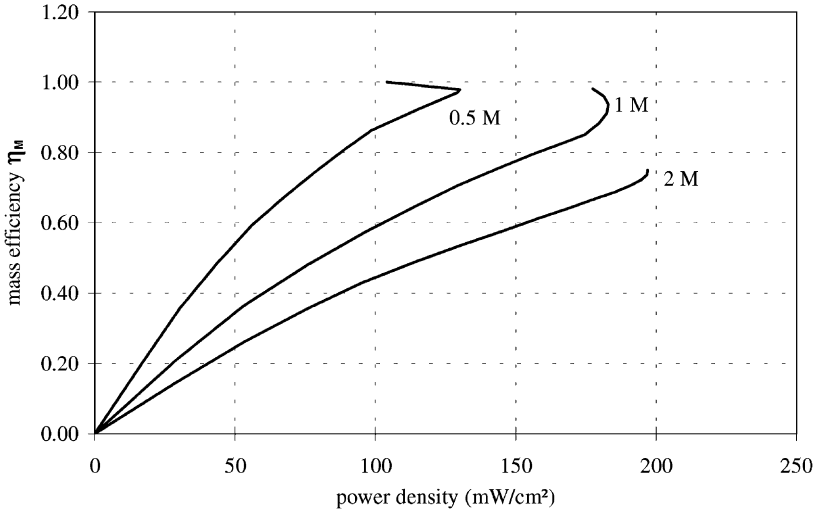

Fig. 6. Mass efficiency (η_M) plotted against power density as a function of methanol concentration. In the partial load range mass efficiencies of >90% can be achieved. At the point of maximum power (full power) the mass efficiency is in the order of 70%.

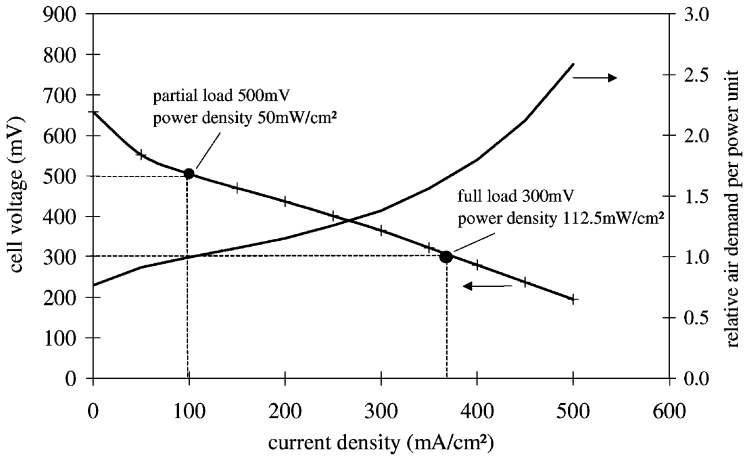

Fig. 7. Relative air demand per power unit as a function of the current density. Same MEA used as in Fig. 4, methanol concentration 1 M. Operating conditions: 85 °C; pressure, 3 bar absolute. Air demand calculated corresponding to Eq. (2.3).

Table 2
Data for the full power and partial power operation

U_C (mV)	I (mA/cm^2)	p_{cell} (mW/cm^2)	N_{air} (mol/(s cm^2))	N_{air}/p_{cell} (mol/(s mW))	Relative air demand
500	100	50	2.48E−6	4.96E−8	1.0
300	375	112.5	9.26E−6	8.24E−8	1.66

The relative air demand is set to 1.0 for the partial power operation. The required air flow (N_{air}) is calculated according to Eq. (2.3) using an air ratio $\lambda = 2$.

the size and the power demand of the air compressor. In Fig. 7, the relative air demand per power unit vs. the current density is plotted. According to Faraday's law, the air consumption is proportional to the electric current. As a reference, the relative air demand is set to 1.0 at a cell voltage of 500 mV (partial load). In examining the current/voltage characteristic, it can be seen that in the full power range the current density is nearly four times higher than in the partial power range whereas the power is only a little bit more than twice as high. This leads to the air consumption in the full power range being 66% higher per unit power as in the partial power range.

Table 2 summarizes the two design points shown in Fig. 7. The air demand (N_{air}) is calculated by Faraday's law (Eq. (2.3)) for an air ratio $\lambda = 2$. The column N_{air}/p_{cell} indicates the required air flow per mW power output. The relative air demand for the partial power ($U_C = 500$ mV) is set to 1.0 as a reference value. In full power operation, the required ratio N_{air}/p_{cell} raises to 8.24E−8 mol/s mW from the initial 4.96E−8 mol/(s mW) which corresponds to an increased relative air demand of 66%. This is an important observation as it has a strong impact on the system efficiency and the compressor power demand.

3.4. Influence of temperature

A temperature range from 60 to 110 °C will be investigated for the following considerations regarding power density and heat flux. On one hand, the temperature influences the electrodes' kinetics [18,19], but at the same time high temperatures lead to an increased water vaporization at the cathode which reduces, e.g. the partial pressure of the oxygen. In addition, in DMFCs the amount of water permeation by electro-osmosis increases with higher temperatures due to swelling effects of the membrane [6].

The additional water is responsible for the decreasing transport properties of both the cathode catalyst and diffusion layer. In general, all these effects lead to a non-linear behavior of the fuel cell power output as a function of the operating temperature T. We experimentally investigated the full and partial power operation in the temperature range between 60 and 110 °C using the same MEAs and the same experimental setup described above.

The results are shown in Fig. 8. The design point partial power operation at 110 °C is taken as a reference with a relative power output being 1.0. The curves of the cell power for the temperature range studied are interpolated linearly in Fig. 8 in the temperature range from 60 to 110 °C with a relatively small error. Additional measurements at 130 °C show that the linearization is not valid for elevated temperatures because of the exponentially increasing electrode kinetics.

The experiments lead to the following assumptions and value ranges for the subsequent system studies:

- a differentiation is made between full and partial power operation;
- mass efficiency in partial power operation (0.9);

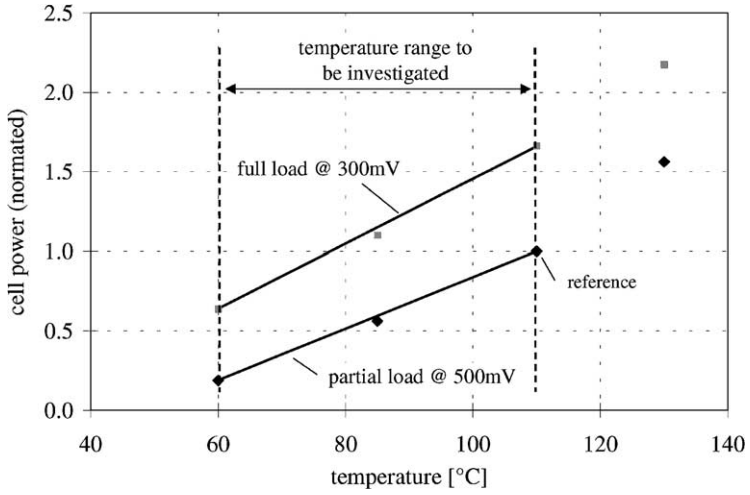

Fig. 8. Influence of cell temperature on cell performance in part and full power operation. The normated cell power is set to 1.0 for the reference point at 110 °C and partial load at 500 mV.

- single cell voltage in partial power operation (500 mV);
- mass efficiency in full power operation (0.7);
- single cell voltage in full power operation (300 mV);
- the temperature range considered is 60–110 °C.

4. System studies

In addition to the parameters studied in Section 3, the air ratio (λ) and the cathode pressure (p) influence fuel cell performance. The influence of the air ratio and the cathode pressure on the stack power is shown in Fig. 9. The system is modeled for a stack power of 1 kW in partial power operation at a stack temperature of 80 °C, an air ratio of 2 and a cathode pressure of 3 bar.

With this system design, the following operation modes are investigated:

- air compressed by a compressor (without expander);
- air compressed by a compressor/expander unit (Fig. 2). In this way part of the stored pressure energy is recovered so that the power required for compression is reduced.

Fig. 10 shows the influence of the air ratio and cathode pressure on the power of the fuel cell stack and of the above-mentioned operation modes.

In full power operation, the compressor's power consumption has a strong effect (Fig. 9). In a system without an expander, at an operating pressure of 4 bar and an air ratio of 4, this results in almost the entire electric power of the fuel cell being consumed for compression of the supplied air. If

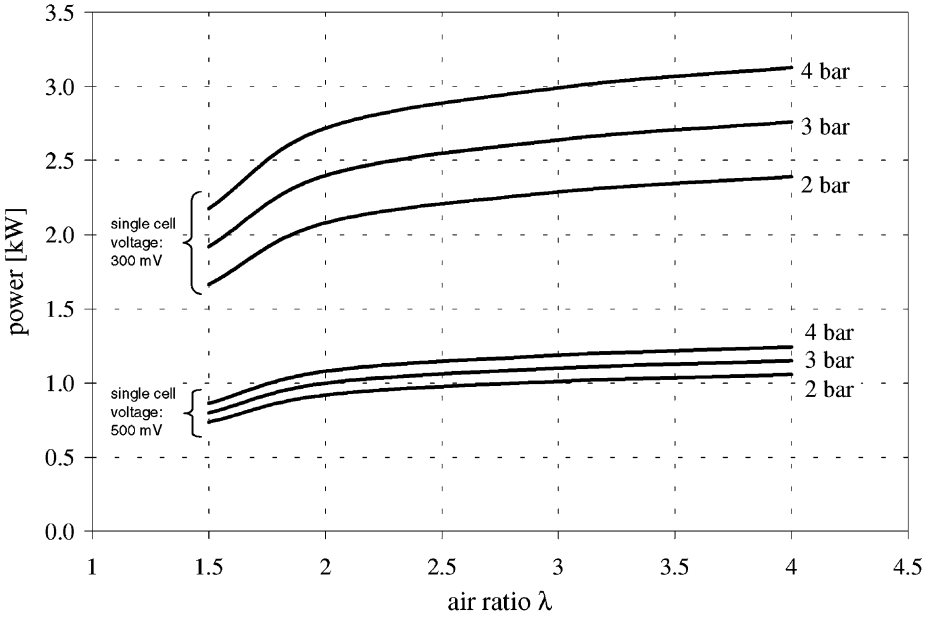

Fig. 9. Influence of air ratio and cathode pressure on the power of a fuel cell stack (modeling assumption).

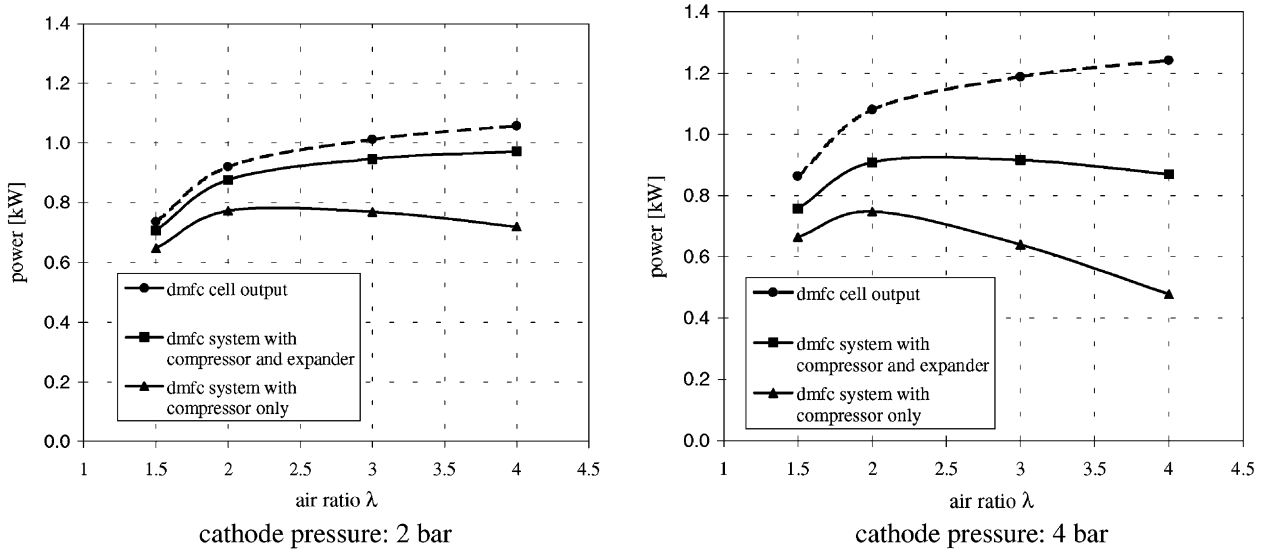

Fig. 10. Influence of the cathode pressure on power in partial power operation (stack temperature = 80 °C).

an expander is used, the power demand of the compressor/expander unit is at a tolerable level when low cathode pressures and air ratios in the range of 2 are applied (Fig. 11). In the following, only systems with a compressor/expander unit for air compression will be studied.

4.1. Electrical system performance and heat power: temperature and pressure

Figs. 12 and 13 show the influence of operating temperature in a temperature range of 60–110 °C on both the heat and the electric power. As expected, the electric power rises with increasing temperature, which also corresponds to the experimental results (Fig. 8). The situation is different with the useful heat power. Depending on the chosen air ratio and cathode pressure, the heat power displays a maximum in both partial power and full power operation. With increasing temperature within the fuel cell stack an increasing vaporization of water occurs within the stack, which causes cooling of the fuel cell stack. Fig. 13 shows that it is impossible to run the stack in partial power operation at 2 bar without additional heating if the operating temperature exceeds 90 °C.

In partial power operation at operating temperatures of more than 90 °C, a cathode pressure higher than 2 bar is necessary in order to obtain a positive heat balance.

Different heat power optima arise for various cathode pressures. The optima are shifted to higher cell temperatures with increasing pressure. In full power operation, the heat power reaches a maximum of approximately 11.5 kW, whereas in partial power operation 1.5 kW is not exceeded. With respect to applications in mobile systems, it is basically

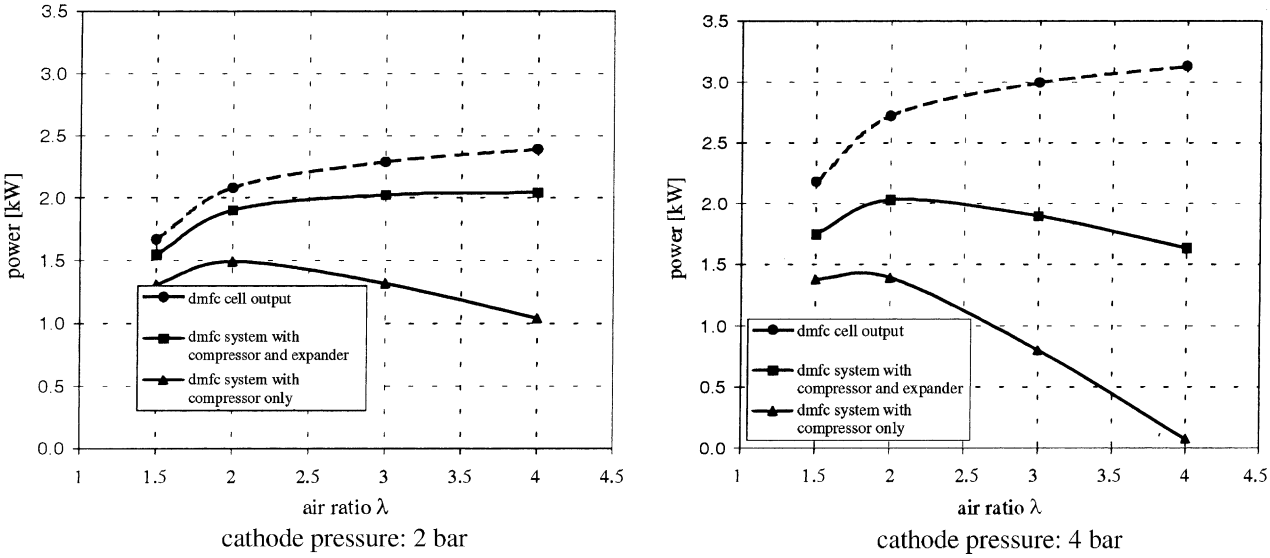

Fig. 11. Influence of the cathode pressure on power in full power operation (stack temperature = 80 °C).

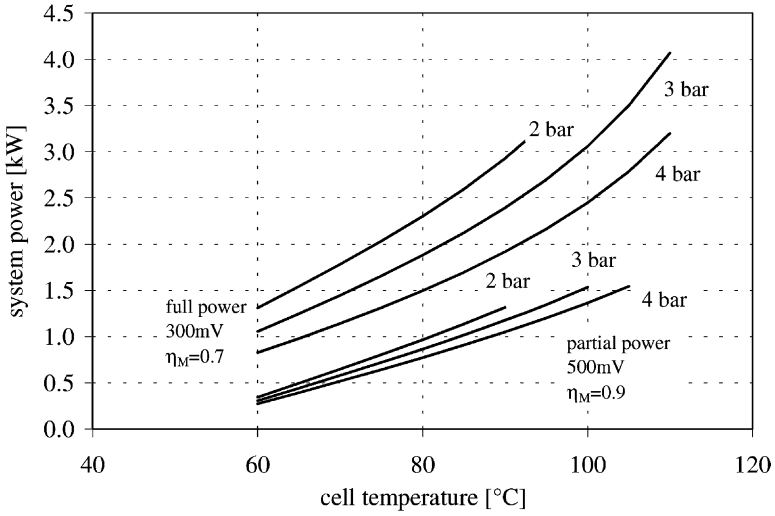

Fig. 12. Influence of temperature and air ratio on the power output of a DMFC system (air ratio, $\lambda = 3$).

desirable to reduce the heat to be extracted in order to keep the dimensions of the cooling system as small as possible. In contrast, for use in stationary units a high amount of useful heat can be beneficial.

4.2. Electrical system power and heat power: temperature and air ratio

Increasing the air ratio leads to increased power consumption by the compressor/expander unit. In analogy to a pressure change, a change in the air ratio has a greater impact during full power operation than with partial power because in partial power operation the air demand is lower.

Increasing temperatures have a greater positive effect on the system power in the case of full power than in the partial power range since the lower efficiencies lead to an increased introduction of heat and tend to result in intensified water vaporization on the cathode side. This increases the useful exhaust gas energy in the expander so that the compressor power to be supplied by the system drops and the system power as a whole increases.

Fig. 14 shows the influence of the air ratio and operating temperature on the useful heat power. Higher air ratios lead to increased water vaporization on the cathode side and thus to a reduction of the quantity of useful heat. In the low temperature range, the partial pressure and thus also the fraction of water vapor in the cathode gas is small, which is why the heat powers achievable for different air ratios become similar.

In partial power operation, the maximum air ratio must not be greater than 2 for operating temperatures above 90 °C at a cathode pressure of 3 bar in order to maintain the temperature.

4.3. Efficiencies

In addition to the absolute values of the system and heat power, the efficiencies are also of interest. The curves of the electrical efficiency and the thermal efficiency run counter to

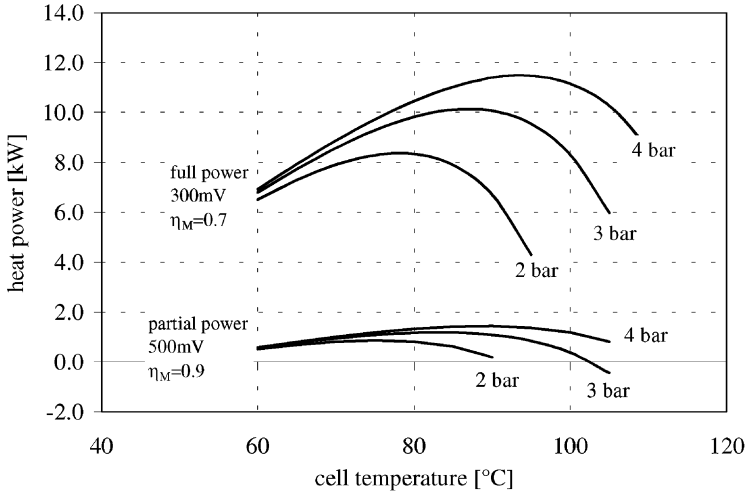

Fig. 13. Influence of operating temperature on the heat power of a DMFC system (air ratio, $\lambda = 3$).

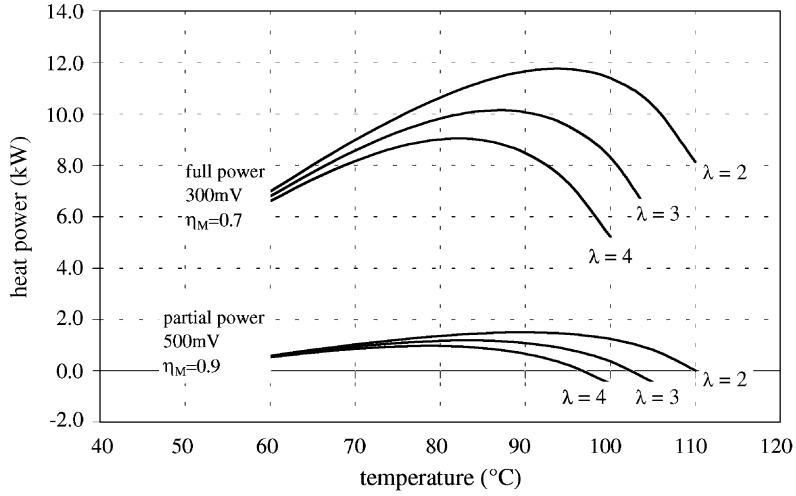

Fig. 14. Influence of temperature and air ratio on the heat power of a DMFC system (cathode pressure = 3 bar).

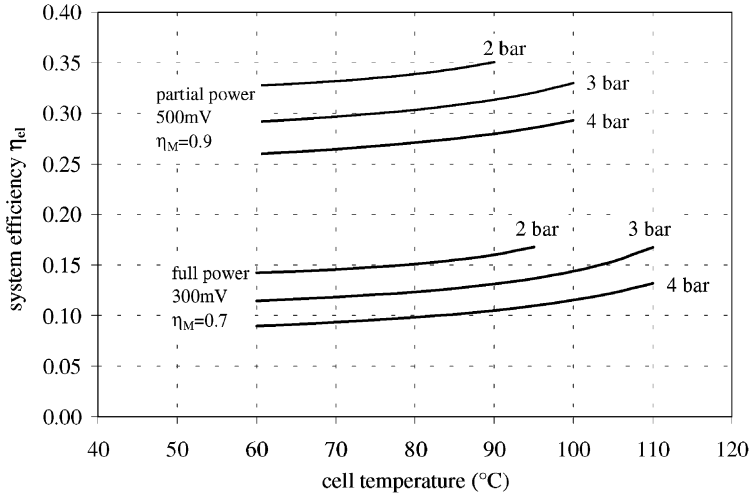

Fig. 15. Influence of operating temperature and cathode pressure on the electrical efficiency of a DMFC system.

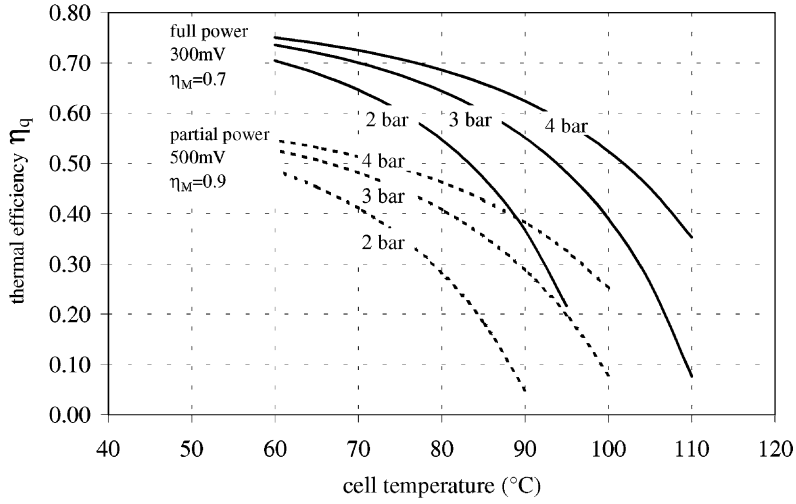

Fig. 16. Influence of operating temperature and cathode pressure on the thermal efficiency of a DMFC system.

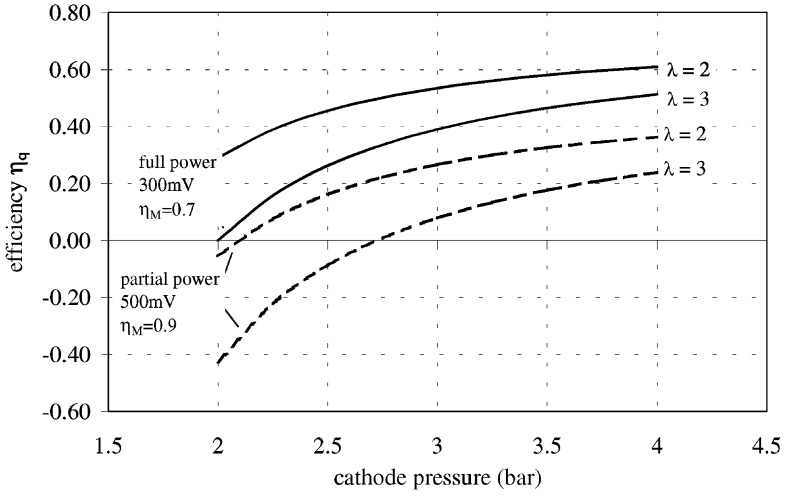

Fig. 17. Influence of cathode pressure and air ratio on the thermal efficiency of a DMFC ($T = 100\ ^\circ C$).

each other with increasing temperature (Figs. 15 and 16). A maximum system efficiency of 35% can be achieved for the partial power range if the cathode pressure is set to 2 bar and the operating temperature to 90 °C.

The achievable system efficiency is lower in the full power range. This is due, on one hand, to the reduced mass efficiency and, on the other hand, to the higher air ratio resulting in increased compressor power. In the full power range the system efficiency is, therefore, restricted to approximately 17%.

Due to vaporization effects at the cathode, the thermal efficiency decreases continuously with increasing temperature. At an operating temperature of 90 °C and a pressure of 2 bar (optimum electrical efficiency), the thermal efficiency is not quite 5% and therefore, just above 0.

With respect to the utilization of heating energy, an elevated cathode pressure is beneficial (Fig. 17). Particularly in the partial power range with higher air ratios and at low cathode pressures, the vaporization enthalpy may exceed the power losses so that it is not possible to maintain the system temperature without additional heating. For an operating temperature of 100 °C in the full power range, a utilization efficiency (η) of 60% can be achieved with an air ratio of 2, whereas approximately 35% is achievable in the partial power range.

5. Conclusions

The present paper is concerned with analyzing the energy and heat management of a DMFC system. The system pressure and the air flow rate have an important impact on both the system power and the system efficiency. Furthermore, the vaporization of water at the cathode influences the heat balance of the cell. In particular, we investigated two design points: full power (300 mV cell voltage) and partial power (500 mV cell voltage) operation. High operating temperatures of the cell, i.e. above 90 °C, require low air flow rates combined with elevated cathode pressures to maintain the temperature.

Cathode pressures in the range of 2 bar and above can only be economically achieved with a compressor/expander unit in which part of the compression work can be recovered in the expander. Increasing pressures lead to an increasing demand of compression power lowering the system efficiency. The decrease of efficiency is more pronounced in the full power range where greater air mass flows occur.

In the partial power range at an air ratio of $\lambda = 3$, a maximum system efficiency of 35% can be achieved. Increasing cathode pressures reduce the efficiency by approximately 4% absolute per bar of pressure. In full power operation with a cell voltage of only 300 mV the system efficiency is considerably lower and, depending on operating conditions, may range from values of approximately 8–16%.

With respect to thermal efficiency, elevated cathode pressures and lower operating temperatures are beneficial since this limits the vaporization of water on the cathode side. In both power ranges studied, increasing the operating temperature leads to a sharp drop in thermal efficiency. In the partial load range the maximum operating temperature which the cell can reach without additional heating is between 100 and 105 °C, depending on the air pressure and the air flow rate.

Since the maximum possible operating temperature of the cell is limited due to the heat balance and water vaporization, the economic success of the DMFC will require the development of MEAs also demonstrating high performance in the relatively low temperature range of 90 °C.

References

[1] K. Kordesch, G. Simader, Fuel cells and their applications, VCH Publishers, Weinheim, 1996.
[2] H. Dohle, H. Schmitz, T. Bewer, J. Mergel, D. Stolten, J. Power Sources 106 (2002) 313.
[3] A. Kindler, T.I. Valdez, C. Cropely, S. Stone, Electrochem. Soc. Proc. 4 (2001) 231.

[4] K. Scott, P. Argyropoulos, W.M. Taama, S. Kramer, K. Sundmacher, J. Power Sources 83 (1999) 204.
[5] P.S. Kauranen, E. Skou, J. Electroanal. Chem. 408 (1996) 189.
[6] X. Ren, W. Henderson, S. Gottesfeld, J. Electrochem. Soc. 144 (1997) 267.
[7] K. Scott, P. Argyropoulos, A. Simoglou, W.M. Taama, in: Proceedings of the International Fuel Cell Conference, Nagoya, Japan, 1999, 137 pp.
[8] K. Scott, P. Argyropoulos, W.M. Taama, J. Power Sources 79 (1999) 169.
[9] H.D. Baehr, Thermodynamik, Springer, Berlin, 1992.
[10] M. Uchida, Y. Aoyama, N. Eda, A. Ohta, J. Electrochem. Soc. 142 (1995) 4143.
[11] A. Havránek, K. Klafki, K. Wippermann, in: Proceedings of the First European Polymer Electrolyte Fuel Cell Forum, Luzern, Switzerland, 2–6 July 2001, 221 pp.
[12] H. Dohle, Ph.D. thesis, RWTH, Aachen, 2000.
[13] H. Dohle, J. Divisek, J. Mergel, H.F. Oetjen, C. Zingler, D. Stolten, J. Power Sources 105 (2002) 172.
[14] R.W. Reeve, P.A. Christensen, A.J. Dickinson, A. Hamnet, in: Proceedings of the 50th ISE Meeting, Pavia, Italy, 5–10 September 1999, 1029 pp.
[15] H. Dohle, J. Divisek, R. Jung, J. Power Sources 86 (2000) 469.
[16] X. Ren, P. Zelenay, S. Thomas, J. Davey, S. Gottesfeld, J. Power Sources 86 (2000) 111.
[17] R.M. Moore, S. Gottesfeld, P. Zelenay, in: Proceedings of the Second International Symposium on Proton Conducting Membrane, Fuel Cells II, Boston, Proc. 98-27 (1998) 388.
[18] P.S. Kauranen, E. Skou, J. Munk, J. Electroanal. Chem. 404 (1996) 1.
[19] B. Beden, F. Kadirgan, C. Lamy, J.M. Leger, J. Electroanal. Chem. 127 (1981) 75.